Atmospheric
Chemistry
and Physics
Discussions

Open Access

Organic aerosol formation from the reactive uptake of isoprene epoxydiols (IEPOX) onto non-acidified inorganic seeds

T. B. Nguyen[1], M. M. Coggon[2], K. H. Bates[2], X. Zhang[1], R. H. Schwantes[1], K. A. Schilling[2], C. L. Loza[2,*], R. C. Flagan[2,3], P. O. Wennberg[1,3], and J. H. Seinfeld[2,3]

[1]Division of Geological and Planetary Sciences, California Institute of Technology, Pasadena, California, USA
[2]Division of Chemistry and Chemical Engineering, California Institute of Technology, Pasadena, California, USA
[3]Division of Engineering and Applied Science, California Institute of Technology, Pasadena, California, USA
*now at: 3M Environmental Laboratory, 3M Center, Building 0260-05-N-17, St. Paul, USA

ACPD

13, 27677–27716, 2013

Organic aerosol formation from the reactive uptake of IEPOX

T. B. Nguyen et al.

Title Page

Abstract	Introduction
Conclusions	References
Tables	Figures

|◄ | ►|

◄ | ►

Back | Close

Full Screen / Esc

Printer-friendly Version

Interactive Discussion

Correspondence to: T. B. Nguyen (tbn@caltech.edu)

Title Page

Abstract | Introduction

Conclusions | References

Tables | Figures

◀ | ▶

◀ | ▶

Back | Close

Full Screen / Esc

Printer-friendly Version

Interactive Discussion

Abstract

The reactive partitioning of *cis* and *trans* β-IEPOX was investigated on hydrated inorganic seed particles, without the addition of acids. No organic aerosol (OA) formation was observed on dry ammonium sulfate (AS); however, prompt and efficient OA growth was observed for the *cis* and *trans* β-IEPOX on AS seeds with liquid water contents of 40–75 % of the total particle mass. OA formation from IEPOX is a kinetically-limited process; thus the OA growth continues if there is a reservoir of gas-phase IEPOX. There appears to be no differences, within error, in the OA growth or composition attributable to the *cis/trans* isomeric structures. Reactive uptake of IEPOX onto hydrated AS seeds with added base (NaOH) also produced high OA loadings, suggesting the pH-dependence for OA formation from IEPOX is weak for AS particles. No OA formation, after particle drying, was observed on seed particles where Na^+ was substituted for NH_4^+. The Henry's Law partitioning of IEPOX was measured on NaCl particles (ionic strength ~ 9 M) to be 3×10^7 M atm^{-1}. A small quantity of OA was produced when NH_4^+ was present in the particles, but the chloride (Cl^-) anion was substituted for sulfate (SO_4^{2-}), suggesting differences in nucleophilic strength of the anions. Online time-of-flight aerosol mass spectrometry and offline filter analysis provide evidence of oxygenated hydrocarbons, organosulfates and, notably, amines in the particle organic composition. The results help explain the substantial quantities of ambient IEPOX-derived OA observed under neutralized conditions. Experiments and models aimed at understanding OA production from IEPOX, or other epoxides, should consider the NH_4^+ activity, in conjunction with H^+ activity (i.e., particle acidity) and nucleophile activity.

1 Introduction

A significant portion of the organic aerosol (OA) production from isoprene, a non-methane hydrocarbon emitted to the atmosphere in vast amounts, is attributed to the heterogeneous chemistry of isoprene epoxydiols (IEPOX) (Froyd et al., 2010; Chan

et al., 2010; McNeill et al., 2012; Surratt et al., 2010; Hatch et al., 2011; Budisulistiorini et al., 2013; Pye et al., 2013). IEPOX, of which there are four isomeric forms (Scheme 1), is a second-generation low nitric oxide (NO) isoprene photooxidation product formed from the OH-oxidation of particular isomers of isoprene hydroxy hydroperoxides (Paulot
5 et al., 2009b). The mechanism for OA production from IEPOX has been proposed as ring-opening of the epoxide group, activated by proton transfer from a strong acid such as sulfuric acid (H_2SO_4), followed by nucleophilic addition of available nucleophiles in the condensed phase, e.g., addition of water to produce tetrols, sulfate to produce organosulfates, and so on (Minerath et al., 2008; Eddingsaas et al., 2010; Surratt et al.,
10 2010). This proposed mechanism has been corroborated by chamber investigations of particle acidity effects on OA formation (Surratt et al., 2007; Lin et al., 2012), wherein dry acidic seeds ($MgSO_4 : H_2SO_4$, 1 : 1) prompted strong reactive uptake behavior from epoxides (Paulot et al., 2009b), compared to negligible uptake for dry, non-acidified seeds.

15 Recent field data suggest that the story might be more complex than described above, as weak correlations between particle acidity and the abundance of IEPOX particle-phase tracer products were observed in Southeastern USA sites (Lin et al., 2013; Budisulistiorini et al., 2013). It should be noted that the indirect definition of "particle acidity," which relies on charge balance of cations and anions, have several lim-
20 itations and may not effectively represent the activity of H^+ in the aqueous phase of particles in some cases (Gregoire, 2013). Nevertheless, from the field observations, Lin and coworkers proposed that other factors may possibly modulate OA formation from IEPOX in conjunction with particle [H^+]. One important distinction between previous chamber investigations, that have all been conducted under dry conditions (relative
25 humidity, RH < 5 %), and the Southeastern USA location is the prevalence of particle liquid water on the ammonium sulfate seeds. Water is a ubiquitous and abundant component of the atmosphere; therefore the effect of liquid water on the uptake of OA precursors has important implications for much of the globe. The crystalline ammonium sulfate seeds used in dry chamber experiments may not have adequate liquid water for

IEPOX to partition into the aqueous phase or sufficient H^+, NH_4^+, and SO_4^{2-} activities to promote reactive uptake. Similarly, a particle with a large weight percent of H_2SO_4 may have a sizeable liquid water component even at RH < 5 % due to the strong hygroscopicity of H_2SO_4 (Xiong et al., 1998), and the difference in reactive uptake of IEPOX

5　may be due either to the differences in particle liquid water or the particle free acidity. In contrast, high concentrations of liquid water may cause dilution of aqueous ions, i.e., changing the acidity or ionic strength, which has been demonstrated to change the effective Henry's Law partitioning coefficient of glyoxal (Kampf et al., 2013). Despite these important interactions, the effect of liquid water on OA formation from IEPOX has

10　not been systematically explored in the laboratory.

　　We report here the reactive uptake of two isomers of IEPOX, the *cis* and *trans* β-IEPOX (Paulot et al., 2009b), which together comprise the dominant majority of the isomer distribution (Bates et al., 2013). We synthesized authentic standards and observed the dark OA growth onto non-acidified and hydrated inorganic seeds at several particle

15　liquid water concentrations. In the atmosphere, ammonium ions (NH_4^+) are one of the most abundant components of aerosols, e.g., (NH_4^+): $1/2 \times (SO_4^{2-})$ or (NH_4^+) : (NO_3^-) ~ 1 (Lin et al., 2013). The aqueous NH_4^+ may possibly act as catalyst for OA formation, as has been shown for a number of atmospherically-important reactions (Noziere et al., 2009; Sareen et al., 2010; Ervens and Volkamer, 2010; Yu et al., 2011). We study reac-

20　tion with NH_4^+ as a potential rate-limiting mechanism for the IEPOX reaction. The role of seed inorganic composition in OA formation is studied by using ammonium sulfate, ammonium chloride, sodium sulfate, and sodium chloride seeds.

2　Materials and methods

2.1　Experimental procedures

25　This work utilized a newly-constructed 24 m^3 FEP Teflon environmental chamber specifically reserved for low-NO$_x$ applications. The walls have not been in contact

with strong acids and the chamber was operated in batch mode. Experiments were performed at room temperature (23–24 °C) and in the dark. Prior to the start of experiments, the chamber was thoroughly flushed with dry, purified air until particle concentrations are $< 0.01\,\mu g\,m^{-3}$. For humid experiments, water vapor was injected until the desired relative humidity (RH) was achieved in the chamber by flowing dry purified air over a Nafion membrane humidifier (FC200, Permapure LLC), which is kept moist by recirculating 27 °C ultra-purified (18 MΩ) water (Milli-Q, Millipore Corp). Temperature and RH were measured by a Vaisala HMM211 probe, calibrated with saturated salt solutions in the RH range of 11–95 %. For RH < 11 %, the water vapor content was quantified by chemical ionization mass spectrometry (Sect. 2.2.1).

Seed particles were injected by atomizing aqueous solutions (0.06 M) of ammonium sulfate ((NH_4)$_2SO_4$, AS), sodium chloride (NaCl), ammonium chloride (NH_4Cl), or sodium sulfate (Na_2SO_4) at 2100 hPa of air into the chamber through a ^{210}Po neutralizer and water trap. All inorganic seeds were injected through a 30 cm custom-built wet-wall denuder kept at 90 °C, such that the seed particles enter the chamber hydrated. Liquid water is expected to evaporate from the seed particles according to the salt's efflorescence behavior (Lee and Hsu, 2000) at the RH of the chamber, e.g., in a dry chamber it is expected that the hydrated particles will enter the chamber fully dried. Particles were allowed to equilibrate until their volume concentrations are stable prior to organic injections.

Two isomers of isoprene epoxydiols (*cis* and *trans* β-IEPOX) were synthesized via procedures adapted from Zhang et al. (2012) and purified with normal-phase column chromatography until the estimated purity based on nuclear magnetic resonance (NMR) spectroscopy of the *cis* and *trans* β-IEPOX isomers are 99 % and > 92 %, respectively. Details of the synthesis and NMR spectra will be forthcoming (Bates et al., 2013). Although the mole fractions of the impurities are low, their high volatility may lead to an over-represented abundance in the gas phase. For the *cis* isomer, we detected experimental interference from the volatile 1,4-dihydroxy-2-methyl-2-butene (a precursor used in the synthesis), comprising ∼50 % of the vapor phase measured directly

above a bulb of IEPOX droplets by chemical ionization mass spectrometer (CIMS, Sect. 2.2). In order to further purify before experiments were conducted, *cis* β-IEPOX droplets were purged with dry N_2, combined with 60 °C heating, for > 8 h until the measured impurity fraction drops below 2 % (Fig. S1, Supplement). After the additional purification, IEPOX was injected into the chamber by flowing a 5–8 L min^{-1} stream of dry purified air past several droplets in a clean glass bulb heated to 60 °C for 2–4 h. The mixtures of IEPOX and seed aerosols were allowed to equilibrate for > 1 h.

2.2 Analytical methods

2.2.1 Chemical ionization mass spectrometry (CIMS)

Gas-phase IEPOX was measured with negative-ion chemical ionization mass spectrometry (CIMS) using CF_3O^- as the reagent ion, described in more detail previously (Crounse et al., 2006; Paulot et al., 2009a; St. Clair et al., 2010). The mass analyzer is a Varian triple-quadrupole spectrometer with unit mass resolution. Air is brought from the chamber using a 3 mm inner diameter perfluoroalkoxy (PFA) Teflon line with flow rate of 2.5 L min^{-1}. Of the total chamber flow, a 145 mL min^{-1} analyte flow was sampled orthogonally through a glass critical orifice into the CIMS. The analyte flow was further diluted by a factor of 12 with dry N_2 to minimize the interaction of water vapor from the chamber with the reagent ion in the ion-molecule flow region. The subsequent data analysis corrects for the dilution factor. The operational pressure and temperature were kept at 35.5 hPa and 35 °C, respectively. The CIMS operated in a scanning MS mode (m/z 50–250) and tandem MS mode (MSMS). In MSMS mode, collisionally-induced dissociation (CID) with 2.6 hPa of N_2 fragments analyte ions into product ions in the second quadrupole, following the ejection of neutral species. The MS cluster ion $C_5H_{10}O_3 \cdot CF_3O^-$ (m/z 203) of IEPOX was used for quantification, due to the higher signal-to-noise (S/N) of this ion compared to MSMS ions. The MSMS product ion $C_5H_9O_3 \cdot CF_2O^-$ ($m/z\,203 \rightarrow m/z\,183$), found to be unique to IEPOX in the isoprene OH-oxidation system, was used to differentiate IEPOX from the isobaric iso-

Organic aerosol formation from the reactive uptake of IEPOX

T. B. Nguyen et al.

prene hydroperoxide (ISOPOOH), which has been documented to yield mainly m/z 63 and a negligible amount of m/z 183 upon CID (Paulot et al., 2009b). ISOPOOH (m/z 203 → m/z 63), was not expected, nor observed, during IEPOX injections.

CIMS calibrations of *cis* and *trans* β-IEPOX were performed by separately atomizing dilute (1–3 mM) solutions of each isomer with equimolar concentrations of hydroxyacetone, used as an internal standard, into the chamber through a 15 cm PFA Teflon transfer line for a few hours. During synthesis, NMR analysis showed that IEPOX was stable in water solution for many hours if no acid was present, so decay of IEPOX in the atomizer solution was not expected over the course of the calibration experiment. Toluene was used as a tracer to obtain the exact volume of the Teflon bag for each calibration experiment. A measured volume of toluene (6 µL) was injected into a clean glass bulb with a microliter syringe (Hamilton) and quantitatively transferred into the chamber with a 5 L min^{-1} stream of dry purified air. The gas-phase toluene was monitored by commercial gas chromatograph with flame-ionization detector (GC-FID, Hewlett-Packard 6890N) using a calibrated HP-5 column (15 m, 0.53 mm i.d.). The initial chamber temperature was 35 °C, and the temperature was ramped until 45 °C or until no increase of IEPOX signal was observed in the CIMS. The atomized solution was weighed before and after atomization. Each sensitivity determination was repeated at least twice. The sensitivities of the IEPOX isomers were calculated from the ratio of the normalized ion counts (with respect to the reagent ion signal) to the number of atomized moles. Small amounts of nucleated organic aerosols were observed in the chamber from the atomization, as measured by a scanning mobility particle sizer (Sect. 2.2.3) and that volume concentration was subtracted from the theoretical moles of IEPOX (corrections of < 1 %). Based on their calculated dipole moments and average polarizability, the *cis* isomer was expected to have a sensitivity of ∼1.4 times greater than the *trans* isomer (Paulot et al., 2009b), and we found the sensitivity of the *cis* isomer to be a factor of 1.8 greater than the *trans* isomer in the MS mode.

Additionally, several mixing ratios of water vapor were introduced into the CIMS ion-molecule region to measure the water dependence of the IEPOX detection. Wa-

ter vapor was quantified by Fourier-transform infrared spectroscopy (FT-IR, Nicolet Magna-IR 560) with a 19 cm pathlength quartz cell. Spectral fitting was performed using the HITRAN spectral database (Rothman et al., 2009) and the nonlinear fitting software NLM4 developed by Griffith (2006). In the low-RH range, outside the calibration limit of the membrane RH probe, the CIMS water ions $H_2O \cdot {}^{13}CF_3O^-$ (m/z 104) and $(H_2O)_2 \cdot CF_3O^-$ (m/z 121) were used to quantify water vapor concentration in the chamber after calibration of water vapor with FT-IR. These ions provide excellent sensitivity to water and linearity in the 20–3500 ppm range in the CIMS ion molecule flow region (corresponding to 1–100 % RH in the chamber at 24 °C, before CIMS dilution). No water dependence in the detection of the IEPOX ions was observed within the range of water vapor observed by CIMS.

In order to quantify the gas-phase concentrations of IEPOX, the CIMS signal was corrected to account for the RH-dependent wall losses of IEPOX. The interactions of IEPOX with chamber walls have not been previously characterized, although those of its C_4 analog have been reported (Loza et al., 2010). IEPOX wall loss experiments were conducted at RH = 3 %, 46 %, and 69 %, as described in Sect. 2.1, continuously for 5–10 h. Figure S2 shows that the wall losses of IEPOX on non-acidic walls were negligibly small ($\sim -0.4 \% h^{-1}$ at RH 69 %), within the error of CIMS measurements.

2.2.2 Aerosol mass spectrometry (AMS)

Online particle composition was measured with a high-resolution time-of-flight aerosol mass spectrometer (ToF-AMS, Aerodyne Research Inc.). The ToF-AMS was operated in V mode ($R \sim 2000$ at m/z 200) and W mode ($R \sim 3000$–4000 at m/z 200). Prior to experiments, the ToF-AMS ionization efficiency was calibrated using size-selected 350 nm ammonium nitrate particles. Gas interferences and elemental ratios were calculated using the fragmentation tables developed by Allan et al. (2004) and Aiken et al. (2008). Data were analyzed in IGOR Pro 6.31 (WaveMetrics, Inc.) using the SQUIRREL v 1.51H and PIKA v 1.10H analysis toolkits. Total concentration of organ-

ics ($\mu g\,m^{-3}$) was calculated by summing the nitrate-equivalent masses of each high-resolution ion correlated with the organic fraction from the V-mode data.

Particles were sampled through a 130 cm Nafion membrane diffusion drier (MD-110, Permapure LLC) to avoid flow obstructions from wet particles, at a flow rate of 0.084 L min^{-1}. It is expected that drying the particles may introduce particle or organic line losses in the drier tube and change the particle bounce characteristics on the AMS vaporizer plate. These perturbations may be corrected by applying a collection-efficiency (CE) factor. It was demonstrated that organic aerosol particles with higher water content have very low bounce probability, which corresponds to a CE of unity (Matthew et al., 2008; Docherty et al., 2013). Comparatively, dry particles have much lower CE ($\sim$0.25 for pure, dry AS) due to the high bounce rate. The CE of IEPOX-derived organic aerosol coated particles was calculated by measuring the mass concentrations of organics, sulfate, and ammonium of the wet particles without a drier, wherein CE was assumed to be unity and line losses assumed to be negligible, and comparing with measurements made through a drier. We observe a CE of 0.75 for all conditions in this work, which is consistent with the collection efficiency of organic aerosols measured previously (Docherty et al., 2013).

2.2.3 Particle size and number concentration (SMPS)

Particle size and number concentrations were measured with a scanning mobility particle sizer (SMPS), comprised of a custom-built differential mobility analyzer (DMA) coupled to a commercial butanol-based condensation particle counter (CPC, TSI Inc.). The SMPS particle size measurement was calibrated with polystyrene latex (PSL) spheres. The particles entering the chamber have a static polydisperse distribution, with peak dry particle diameter distributions in the range of 50–100 nm. The sample air flow was not dried in humid experiments. Particle mass concentrations were corrected for RH- and size-dependent wall losses. The mass concentration of particles typically ranged from 65–90 $\mu g\,m^{-3}$ for all experiments, using a particle density of 1.2 g cm^{-3}.

For AS-based experiments, the particle liquid water content was calculated based on the size-dependent hygroscopicity of AS (Biskos et al., 2006; Hu et al., 2010). For each particle diameter bin measured by SMPS, a theoretical dry diameter was calculated based on literature growth factor data at the RH of the experiment. The difference in the wet (measured) and dry (calculated) integrated area of the mass distribution yielded the liquid water concentration in $g\,m^{-3}$. Similarly, the percent liquid water content is calculated as $\%\,LWC = 100\,\% \times (V_{wet} - V_{dry})/V_{wet}$, using the predicted wet and dry diameters.

Particle wall loss characterizations were performed for AS seeds at RH = 3 %, 20 %, 50 %, and 80 % prior to the start of the experimental series to correctly quantify the mass concentrations of particles as a function of time. It was assumed that the loss rates of AS were representative for particles of different composition. Seed aerosols were atomized into the dry or humid chambers in the dark, allowed to stabilize, and particle size and number concentrations were measured for > 12 h. The particle correction method that accounts for wall loss has been discussed in detail previously (Loza et al., 2012).

2.2.4 Filter collection and analysis

Offline OA composition analysis was performed by ultra-high performance liquid chromatography time-of-flight electrospray ionization mass spectrometry (UPLC/ESI-ToFMS). Aerosol samples were collected onto Teflon membrane filters (Millipore, 1 μm pore), pulled at a 20 L min^{-1} flow through an activated charcoal denuder to remove the volatile and semivolatile components. Each filter was extracted with methanol (Fisher, Optima grade, $\geq$ 99.9 %) by ultrasonication for 15 min in a 20 mL scintillation vial. The filtered extracts were blown dry under a gentle stream of ultra-high-purity N$_2$. The residue was reconstituted with 150 μL of 50 : 50 v/v acetonitrile (Fisher Optima grade, $\geq$ 99.9 %) and water (Milli-Q).

Extracts were analyzed by a Waters Xevo G2-S UPLC/ESI-ToF-MS equipped with an Acquity CSH C18 column (1.7 μm, 2.1 mm × 100 mm). The solvents used for gradi-

ent elution were acetonitrile (Fisher Optima grade, $\geq$ 99.9 %) and water with a 0.1 % formic acid spike (solvent "A"). The flow rate was held at 0.5 mL min^{-1}. Accurate mass correction was completed by a lock spray of leucine enkephalin (0.61 ng µL^{-1} in 50 : 50 v/v acetonitrile/water with 0.1 % formic acid). The ESI source was operated in negative mode, where most analytes are ionized by deprotonation and measured as [M-H]$^-$. Ionic molecular formulas were determined from accurate masses (mass resolution of 60 000 at m/z 400) using the elemental composition tool in Mass Lynx. Control filters (no particles) and laboratory controls (seeds only) were analyzed in the same manner.

3   Results and discussion

3.1   Reactive uptake of *cis* and *trans* β-IEPOX onto ammonium sulfate seeds

3.1.1   Liquid water content of seeds

Figure 1 shows the time profile for the organic aerosol (OA) growth corresponding to reactive uptake of the *trans* β-IEPOX onto ammonium sulfate (AS) seeds at two RH conditions, dry (LWC $\sim$ 0 %) and RH 57 % (LWC $\sim$ 55 %). The traces shown in Fig. 1 are representative of uptake behavior for both isomers on the experimental timescale. For RH conditions above the ammonium sulfate (AS) efflorescence point tested in this work ($E_{RH} \sim$ 35 %, (Biskos et al., 2006)), prompt and efficient OA growth onto AS seeds was observed for both IEPOX isomers. No OA growth was observed when the AS seeds were dry, in good agreement with other reports (Lin et al., 2012; Surratt et al., 2010).

The OA growth from IEPOX did not halt after the end of the gas-phase injection period (Fig. 1, solid black line), even after periods of > 2 h (Fig. S3, top panel). This behavior is indicative of a non-equilibrium process, as the addition of nucleophiles is not reversible after the rate-limiting step of IEPOX activation (Eddingsaas et al., 2010). The formation of low-volatility compounds should continue as long as a reservoir of gas-phase IEPOX is available. The series of expected reactions leading to the formation of

ring-opening products (ROP) is shown below, illustrated using a general proton donor (AH) and nucleophile (Nu):

$$IEPOX_{(g)} \leftrightharpoons IEPOX_{(aq)}; K_H \tag{R1}$$
$$IEPOX_{(aq)} + AH \leftrightharpoons IEPOX\text{-}H^+ + A_{-H}; k_{AH} \tag{R2}$$
$$IEPOX\text{-}H^+ + Nu \rightarrow ROP\text{-}H^+; k_{Nu} \tag{R3}$$
$$ROP\text{-}H^+ + A_{-H} \rightarrow ROP + AH; k_{neutral} \tag{R4}$$

For a solution with low AH and Nu activity, the equilibrium accommodation of IEPOX into the aqueous phase, described by the Henry's Law coefficient of IEPOX (K_H), can be measured in isolation. Henry's Law is not an appropriate description of the IEPOX reactive uptake on the liquid water of suspended aerosols, as the aerosol water layers represent highly non-ideal solutions and the OA formation is kinetically-limited. The OA formation mechanism may include contributions from reactions other than Reactions (1–4). To a first-order approximation, total OA mass formed from gas-phase reactive uptake of IEPOX will be a function of aqueous IEPOX concentration, nucleophile activity, and catalyst activity.

For the sake of comparison between experiments, it is useful to have a metric that includes the ratio of OA formed to gas-phase IEPOX injected and accounts for the variability in the size and number of injected seeds between experiments, which is reflected by the calculated aerosol water at different RH. We define here a reactive partitioning coefficient ($\Phi_{OA/IEPOX}$), calculated similarly to an effective Henry's Law coefficient, and thus having the same units (Seinfeld and Pandis, 2006):

$$\Phi_{OA/IEPOX} = (C_{OA}/C_{IEPOX})/[10^{-6} \cdot R \cdot T \cdot P_{LWC}] \tag{1}$$

where (C_{OA}/C_{IEPOX}) is the mass concentration ratio of the IEPOX-derived organic aerosol (dried), measured by ToF-AMS, and the gas-phase IEPOX, measured by negative-ion CIMS; P_{LWC} is the liquid water content of the inorganic aerosols prior to IEPOX introduction ($g\,m^{-3}$); R is the ideal gas constant ($atm\,L\,mol^{-1}\,K^{-1}$); T is the

temperature (K); and 10^{-6} is a conversion factor ($\mathrm{m^3\,cm^{-3}}$). $\Phi_{\mathrm{OA/IEPOX}}$ includes the contribution from Henry's Law equilibrium partitioning of IEPOX (Reaction 1), and thus is an upper limit for the effective Henry's Law coefficient.

We observe that $\Phi_{\mathrm{OA/IEPOX}}$ was not time-dependent when both IEPOX and OA are increasing, as the ratio $C_{\mathrm{OA}}/C_{\mathrm{IEPOX}}$ stabilized when OA grows in response to gas-phase IEPOX (Fig. S3) but increased after IEPOX injection stops. The stabilized ratio is used for $\Phi_{\mathrm{OA/IEPOX}}$ calculations to compare between experiments. P_{LWC} did not have a significant time-dependence due to a stable particle volume distribution before IEPOX gas-phase injections. The uncertainty in the accuracy of the $\Phi_{\mathrm{OA/IEPOX}}$ measurements was estimated to be 50 %, compounded from the uncertainties in the calculated CIMS sensitivities, liquid water fraction, AMS organic mass determinations, and other measurements.

A summary of $\Phi_{\mathrm{OA/IEPOX}}$ and other values is given in Table 1 for all AS-based uptake experiments. Figure 2 shows $\Phi_{\mathrm{OA/IEPOX}}$, as a function of particle liquid water, for the *cis* and *trans* β-IEPOX uptake onto hydrated AS. A trend of decreasing $\Phi_{\mathrm{OA/IEPOX}}$ with increasing LWC was reproducibly observed, despite the uncertainty range in the $\Phi_{\mathrm{OA/IEPOX}}$ determinations. The suppression of $\Phi_{\mathrm{OA/IEPOX}}$ as a function of added water is likely due to dilution. For example, high aerosol sulfate concentrations may cause a "salting-in" effect for IEPOX, or other water-soluble organic compounds (Kampf et al., 2013), which is inversely proportional to water content. Higher water may also reduce the [H$^+$], although the dependence of the reaction on catalyst concentrations is not expected to be high. Additionally, higher P_{LWC} dilutes the aqueous IEPOX and nucleophile concentrations in the aerosol liquid water, which reduce the rate of the chemical reaction as these species are direct reagents. The dilution effect from increasing the pure water fraction at a fixed ion content (moles of $\mathrm{NH_4^+}$ and $\mathrm{SO_4^{2-}}$) is in contrast to a modeled increase in OA formation in areas with high "anthropogenic water", i.e., mixtures of water-soluble compounds found in urban regions (Carlton and Turpin, 2013). In the atmosphere, the partitioning of anthropogenic gases like $\mathrm{NH_3}$ and $\mathrm{SO_2}$ will si-

multaneously impact aqueous acidity and inorganic concentration and thus may lead to enhanced OA formation in areas with higher P_{LWC}.

3.1.2 Particle acidity

As the decrease of $\Phi_{OA/IEPOX}$ with increasing liquid water content may be due to more than one factor, an experiment was carried out to isolate the effect of pH. In experiment 9 (Table 1), the AS solution was neutralized with a strong base (NaOH) until the atomizer solution reached pH = 7. Solutions of AS without additives had pH ~ 5.5 before atomization because, although no strong acid was present, H^+ is expected to be present in small quantities based on the dissociation equilibria of inorganics and dissolution of CO_2. An enhancement in the acidity of the particle may result from a smaller volume of water in the particle and/or through loss of NH_3 upon atomization. In the case of a fully-hydrated AS particle, the pH in the particle is predicted to be pH ~ 4 using the E-AIM Model (Clegg et al., 1998), and modeled pH values in the particle for all AS-based experiments are shown in Table 1. When the RH is below the deliquescence point of AS, the pH was estimated by assuming a dilution due to the calculated P_{LWC}. It is expected that atomization will also lead to slightly lower pH for the base-neutralized atomizer solution, so the particle may have pH < 7. However, adding NaOH above neutralization to counter this effect may induce side reactions such as base-catalyzed epoxide opening and OH^- nucleophilic addition (Solomons and Fryhle, 2004). NaOH is not explicitly treated in the E-AIM and AIOMFAC (Zuend et al., 2008) inorganic models; therefore, it was assumed that atomization of the AS + NaOH solution may lead to, at most, the same enhancement factor that occurred for the pH of the pure AS solutions.

Figure 3 shows that $\Phi_{OA/IEPOX}$ for the *trans* β-IEPOX + AS system decreases slightly as pH is increased, reaching a plateau above pH ~ 4. We note that any perceived change is within the error of the measurement; however, it is clear that the trend of $\Phi_{OA/IEPOX}$ with pH is minor. These results differ from those of Eddingsaas et al. (2010), who observed a linear increase of epoxide reaction rate with H^+ activity. Eddingsaas et al. used H_2SO_4/Na_2SO_4 solutions, and thus the differences in observations may be

entirely due to the high NH_4^+ activity in the AS particles employed in this work. The data suggest that when $[H^+]$ is small, NH_4^+ may activate reactions leading to OA formation, similarly to its catalytic activity toward glyoxal (Noziere et al., 2009), methylglyoxal (Sareen et al., 2010), and other carbonyls (Nguyen et al., 2013; Bones et al., 2010). Interestingly, pH > 4 is the range where NH_4^+ catalysis is most efficient. This is demonstrated by a stable reactivity of the NH_4^+-catalyzed reaction to generate brown carbon from limonene SOA at pH 4–9, but a sharp decline of reactivity below pH 4 (Nguyen et al., 2012). As the H^+ and NH_4^+ ions are reactive toward organics in low-moderate and moderate-high pH ranges, respectively, the resulting pH dependence may appear to be weak in AS-containing seeds. The dual reactivities of H^+ and NH_4^+ toward IEPOX is expected to be important in nature, as NH_4^+-based seeds are abundant.

In comparison, the $MgSO_4 : H_2SO_4$ particles at RH < 5 % in the work of Lin et al. (2012) are strongly acidic. These particles are predicted to have a non-negligible amount of water due to the large hygroscopicity of H_2SO_4 – and indeed, acidity in particles is not a useful concept if water is not present. At RH = 1–5 %, pure H_2SO_4 particles have a growth factor of 1.1–1.2 (Xiong et al., 1998). Assuming a growth factor of 1.15, and taking into consideration the inorganic seed mass concentration, we calculated P_{LWC} for the mean results in Lin et al. (2012), shown in Table 1. The AIOMFAC Model (Zuend et al., 2008, 2011) was used to estimate the pH based on the molal activity of H^+ in the $MgSO_4 : H_2SO_4$ (1 : 1) particle. The calculated pH is ~ -10 and the corresponding mean $\Phi_{OA/IEPOX}$ is $\sim 1.5 \times 10^8$ M atm^{-1} for *cis* β-IEPOX (the *trans* isomer was not studied). $\Phi_{OA/IEPOX}$ for the acidic $MgSO_4$ seeds is slightly higher than, but within the error of, the $\Phi_{OA/IEPOX}$ values for non-acidified AS seeds when a small amount of water is present (RH ~ 40 %). This comparison is meant to be qualitative and subject to uncertainty because the experiments were not performed under the same conditions. Nevertheless, the comparison shows that a solution of high H^+ activity and a solution of high NH_4^+ activity may both lead to a relatively-similar reactive uptake. As $[NH_4^+] \gg [H^+]$ in the particles in this work, a similar $\Phi_{OA/IEPOX}$ would also suggest that $k_{NH_4^+} \ll k_{H^+}$ if

Organic aerosol formation from the reactive uptake of IEPOX

T. B. Nguyen et al.

Title Page

Abstract	Introduction
Conclusions	References
Tables	Figures

|◄| ►|
◄ ►

Back | Close

Full Screen / Esc

Printer-friendly Version

Interactive Discussion

the observed rate coefficient for Reaction (2) is defined as $k_{obs} = k_{AH} \cdot [AH]$. Eddingsaas et al. (2010) estimated k_{H^+} to be $\sim 5 \times 10^{-2}$ M^{-1} s^{-1} for IEPOX.

3.2 Molecular picture of OA formation from IEPOX

3.2.1 Cation and anion substitutions

To further investigate the role of NH$_4^+$ in IEPOX ring-opening reactions at near-neutral conditions, NH$_4^+$ was replaced by a cation that cannot act as a proton donor (Na$^+$). As isomer structure appears to be unimportant for uptake, only the *trans* isomer was used for this portion of the study. Further, many nucleophiles present in the atmosphere are known to add to the protonated epoxide to give the beta-hydroxy ring opening product; for example: H$_2$O (Solomons and Fryhle, 2004), SO$_4^{2-}$ ions (Cavdar and Saracoglu, 2009), NH$_3$ or amines (Clayden et al., 2001), and halide ions (Clayden et al., 2001). Thus, SO$_4^{2-}$ was substituted by Cl$^-$ to study the anion (or nucleophile) effect.

Hydrated particles of AS ((NH$_4$)$_2$SO$_4$), sodium sulfate (Na$_2$SO$_4$), ammonium chloride (NH$_4$Cl), and sodium chloride (NaCl) were introduced into the chamber in separate experiments, followed by the introduction of *trans β*-IEPOX. The mixtures were allowed to equilibrate for 3.5–6 h. The RH range for these reactions is 60–85 %, chosen at a point well above the efflorescence RH of the salts (Martin, 2000), so that each seed would contain a considerable fraction of liquid water. The particle size distributions for each seed type were polydisperse and unimodal, with hydrated mobility diameters in the range of 15–600 nm and with 60–120 nm peak diameters. It is expected that the hydrated particles were spherical. The size-dependent hygroscopicities of AS and NaCl are well-studied; however, the calculations of liquid water content for other seed types are subject to error based on the method we described due to limited literature data. Therefore, we opt to present results based only on the C_{OA}/C_{IEPOX} for the comparison of inorganic seed compositions.

OA formation after particle drying, as detected by ToF-AMS, is negligible for both sodium salts (NaCl and Na$_2$SO$_4$). The OA mass did not grow in response to the ad-

dition of IEPOX for the Na$^+$-based particles (Fig. S4). Figure 4 shows the average stabilized ratios of OA formed with respect to *trans β*-IEPOX injected for the four inorganic salts used in this work. The atomizer solution pH for Na$^+$-based seeds was also ~5.5, a typical pH for a water solution in equilibrium with CO$_2$ (Reuss, 1977). The large

5 difference in reactivity of IEPOX on Na$_2$SO$_4$ vs. (NH$_4$)$_2$SO$_4$ seeds may be attributed primarily to NH$_4^+$ activity, although there will be some differences in [H$^+$] for the NH$_4^+$-based and Na$^+$-based seeds due to the slight dissociation of NH$_4^+$ ⇆ NH$_3$. Additionally, in light of the weak pH-dependence for AS solutions, it appears likely that NH$_4^+$ activity is an important factor in suppressing OA formation on Na$_2$SO$_4$ seed particles. The results

10 show that equilibrium partitioning of IEPOX, i.e., any condensed-phase mass formed from unreacted IEPOX, onto salty solutions is not competitive with reactive partitioning for OA formation.

For the ammonium salts, NH$_4$Cl produced an order of magnitude lower mean C_{OA}/C_{IEPOX} ratio than (NH$_4$)$_2$SO$_4$, after an approximate 2 h delay (Fig. S4). The mod-

15 eled pH, using E-AIM, for both ammonium salt systems is similar (pH ~ 4–4.5), and thus, the difference in reactivity is attributed to the nucleophilic activity of Cl$^-$ compared to SO$_4^{2-}$. Interestingly, Minerath et al. (2009) showed that acid-catalyzed ring opening products of an epoxide with Cl$^-$ may be more efficient than SO$_4^{2-}$. In that study, sulfuric acid was added to the NaCl + epoxide aqueous solution, which provide sulfate and

20 bisulfate ions to the solution. Therefore, the results may not be directly comparable to this work. Furthermore, if Cl$^-$ can be a good nucleophile (poor leaving group) when coupled with NH$_4^+$ catalysis, we would expect to observe organochloride products because hydrolysis at the low-acidity conditions in this work will be slow. There was no evidence of organochloride-derived accurate mass fragments in ToF-AMS data for the

25 NH$_4$Cl reactive uptake organics.

3.2.2 Henry's Law coefficient

Although ToF-AMS did not observe OA formation for experiments using sodium salts (NaCl and Na_2SO_4), the wall-loss-corrected SMPS data (not dried) showed a minor and stable change in particle volume upon injection of IEPOX into the chamber with hydrated NaCl or Na_2SO_4 seeds (Fig. S5a, shown for NaCl). It is likely that the dissolved, but un-reacted, IEPOX was removed from the condensed phase upon particle drying, which would lead to no observed OA mass in the ToF-AMS data throughout the duration of the experiment. The reversibility OA formation on the hydrated Na^+-based seeds indicates equilibrium-partitioning of IEPOX into the aerosol liquid water. The ratio of dissolved OA to injected IEPOX (Fig. S5b) reached a steady-state value at the end of the IEPOX injection period. Because NH_4^+ is not present, and $[H^+]$ is not expected to be considerable in the aqueous phase, Reactions (2) and (4) are unimportant for this system. Further, in experiments using NaCl seeds, where the nucleophilicity of the solution is weaker, we are able to neglect the contribution of Reaction (3), thereby isolating the equilibrium partitioning of IEPOX (Reaction 1).

We estimate the Henry's Law coefficient (K_H) for the equilibrium partitioning of IEPOX into a briny liquid (NaCl ~ 9 M ionic strength) representative of atmospheric aerosol: $K_H = 3 \times 10^7 \, (\pm 50\%) \, \mathrm{M \, atm^{-1}}$. The K_H in a solution of NaCl may be different than the value in pure water, due to complex aqueous interactions of Cl^- and Na^+ with water-soluble organics. As an example, the Henry's Law coefficient for glyoxal was measured to be $K_H = (4.19 \pm 0.87) \times 10^5 \, \mathrm{M \, atm^{-1}}$ in pure water, $1.90 \times 10^6 \, \mathrm{M \, atm^{-1}}$ in a 0.05 M NaCl solution, and $8.50 \times 10^5 \, \mathrm{M \, atm^{-1}}$ in a 4.0 M NaCl solution at 298 K (Ip et al., 2009). Ip et al. (2009) attributed the increase in K_H for NaCl solutions at low ionic strengths to hydrogen bonding interactions of Cl^- and OH groups and the decrease at high ionic strength to a "salting-out" effect. The K_H value for IEPOX has not been experimentally determined in the past; however, the range of K_H has been estimated using the HENRYWIN model (EPA, 2008) by several studies. For example, Eddingsaas et al. (2010) estimated $K_H = 2.7 \times 10^6 \, \mathrm{M \, atm^{-1}}$, using a bond contribution method, and

$K_H = 2.9 \times 10^{10}\,\mathrm{M\,atm^{-1}}$, using a group contribution method in version 4.0 of the model. The empirical K_H value reported here is within range of both estimations – closer to the bond contribution method estimate. These results provide a critical constraint in the partitioning coefficient, significantly decreasing the error associated with using K_H in a quantitative manner (from 4 orders of magnitude to ~50 %).

3.2.3 Organic composition

A full analysis of the OA composition is outside the scope of this work. The reader is referred elsewhere for a discussion of the formation of oxygenated hydrocarbons, e.g., tetrols, alkenetriols, and organosulfates in the aqueous reaction of IEPOX catalyzed by acidic sulfate (Eddingsaas et al., 2010; Surratt et al., 2010). Although strong acid is absent in the systems studied in this work, we observe many similarities in the IEPOX-derived OA composition compared to the published chamber and field results. For example, organosulfates products are abundant. The dominant ion observed in negative ion mode UPLC/ESI-ToFMS for AS uptake is $C_5H_{11}SO_7^-$ (Fig. S6), corresponding to the ring-opening trihydroxy organosulfate product of IEPOX. Derivatization was not performed in this work to detect tetrols. Organosulfate fragments were also observed in ToF-AMS (CSO family of fragments, not shown).

The ToF-AMS data indicate that the IEPOX-derived OA formed under near-neutral conditions in this work have composition similar to OA observed in the field. The suggested field tracers for IEPOX-derived organics, m/z 53 (mostly $C_4H_5^+$) and m/z 82 (mostly $C_5H_6O^+$) (Lin et al., 2012; Robinson et al., 2011; Budisulistiorini et al., 2013), were observed in uptake experiments using both isomers. These mass fragments were proposed to originate from the electron-impact (EI) ionization of furan-derived molecules that might be formed from the acid-catalyzed rearrangement of IEPOX (Lin et al., 2013). Figure 5 shows the difference between mass spectra at the end of the experiment and those at the time period prior to organic injection, corresponding to the organic fraction of the OA formed from the uptake of both isomers. The spectral

ion distributions are very similar to each other and m/z 53 and m/z 82 constituted a substantial fraction of the total ion intensity. The ion abundance of tracer fragments increased in accordance to the growth of OA mass (Fig. S7). As m/z 53 ($C_4H_5^+$) is a reduced fragment, it is also linked to hydrocarbon-like organics in chamber studies and may not be unique to IEPOX-derived OA. m/z 53 was observed in all experiments, including those that used Na^+-based seeds. However, m/z 82 is abundant only when NH_4^+-based seeds were used, supporting the suggestion that it is formed though the EI fragmentation of an IEPOX-derived ring-opening product in ToF-AMS.

A unique aspect of the NH_4^+-catalyzed ring opening reaction of IEPOX is the minor possibility of nucleophilic addition by NH_3, instead of reforming NH_4^+ after neutralizing the addition of another nucleophile. Figure 6 shows ion peaks for organic fragments containing C–N bonds observed in ToF-AMS data from the uptake of *trans* β-IEPOX onto AS vs. Na_2SO_4 seeds. The same C–N fragments were observed in *cis* β-IEPOX experiments using AS. These C–N fragments were not initially present in the AS seeds, and grow linearly following the introduction of IEPOX. Individual C–N fragments correlate well (Fig. S8, linear fit R^2 = 0.69–0.88) with the m/z 82 IEPOX-derived OA tracer fragment ($C_5H_6O^+$), suggesting that reaction of IEPOX is responsible for the presence of these amines. Comparatively, C–N type fragments were negligible or non-existent in uptake experiments from Na^+-based seeds. To the best of our knowledge, this is the first evidence of amine formation from IEPOX. As organic nitrogen compounds also give rise to non-nitrogenous mass fragments in ToF-AMS, it is not possible to estimate a mass concentration for the amines in this work. However, the C–N family of fragments comprised approximately 10 % of the $C_5H_6O^+$ signal, an indication that amine formation may not be negligible. The formation of organic nitrogen from the IEPOX + NH_4^+ reaction has important implications in the atmosphere as the ring opening reaction of epoxides with amines should be more efficient than with NH_3 (Azizi and Saidi, 2005). Further investigations may provide more insight on the source of organic nitrogen from the atmospheric reactions of epoxides.

4 Summary and atmospheric implications

It was demonstrated here that the conversion of IEPOX to organic aerosol (OA) depends on the coupled relationship between the inorganic composition and liquid water content of the particle (P_{LWC}). The inorganic composition governs the catalyst and nucleophile characteristics, and P_{LWC} provides a reaction medium for the partitioning of IEPOX and controls the activities of all the aqueous components. We showed that the equilibrium partitioning (Reaction 1) and the rate-limiting step of IEPOX activation (Reaction 2) do not proceed in the absence of liquid water; however, increasing P_{LWC} does not necessarily increase the reactive partitioning coefficient due to various dilution effects. When the inorganic particle is hydrated, the OA conversion is then determined by the catalyst and nucleophile activities. The rate of OA formation incorporates both Reactions (2) and (3), as illustrated by the cation and anion substitution case studies. In the hydrated Na_2SO_4 experiment, there was high activity of a relatively-good nucleophile, but a good catalyst was absent. Therefore, the formation of OA, i.e., the ring-opening product, was not observed because the equilibrium of Reaction (2) favors $IEPOX_{(aq)}$. The aqueous IEPOX mass that partitioned from the gas phase (K_H) onto the hydrated Na^+-based seeds was removed from the condensed phase following the evaporation of water. In the hydrated NH_4Cl experiment, there was high activity of a good catalyst but a poor nucleophile. A smaller quantity of OA formed because the rate of Reaction (3) was slow, which was further supported by the observed 2 h delay in OA formation. Only when P_{LWC}, NH_4^+ activity, and SO_4^{2-} activity are all significant, as in the case of hydrated $(NH_4)_2SO_4$ seeds, is the OA formation efficient and prompt. OA mass formed from IEPOX uptake onto 1 : 1 $MgSO_4$: H_2SO_4 seeds (RH < 5 %) may also be explained in terms of these conditions, as $P_{LWC} \sim 30$ %, and consequently, both H^+ and SO_4^{2-} activity were high in the particle.

In the atmosphere, relationships of water-soluble OA formed with P_{LWC} may be different and more difficult to interpret compared to laboratory studies because an increase in the P_{LWC} of atmospheric particles is often accompanied by the co-partitioning of

water-soluble organic and inorganic compounds. The abundance of water-soluble organic compounds in the Southeast USA has been observed to be proportional to the liquid water contents of particles (Hennigan et al., 2008, 2009; Carlton and Turpin, 2013). In contrast, a weak correlation of modeled P_{LWC} with the abundance of IEPOX-derived OA tracers has also been observed, in the same geographical region (Budisulistiorini et al., 2013). The results of this work may not be directly comparable to field observations; however, they do not necessarily conflict. Particles may experience multiple hydration/dehydration cycles in the atmosphere, and the majority of particles likely contain liquid water at some point during their long lifetimes. The OA produced from IEPOX reactive uptake onto AS is irreversible (not removed from particle drying in this work), and depending on whether it had been sampled in the atmosphere before or after a dehydration cycle, the apparent correlation of IEPOX-derived OA with P_{LWC} would be different. Consequently, systematic studies in the laboratory are important in elucidating observations from the field.

Our results offer an alternate explanation to the abundance of IEPOX-derived OA tracers when the free H^+ acidity in particles is modeled to be low (Lin et al., 2013). It has been suggested that the reason for the weak correlation with acidity is the reaction of an acidic seed particle with IEPOX to form organosulfates, which affects the particle acidity over time (Budisulistiorini et al., 2013). We show here that particle acidity does not appear to be important for OA formation on hydrated $(NH_4)_2SO_4$ seeds. This result suggests that the OA formation process from IEPOX is insensitive to changes in the degree of neutralization of the particles in many AS-dominated areas, including the Southeast USA. The typical $[NH_4^+]$ is several orders of magnitude larger than $[H^+]$ in atmospheric particles, making it very likely to activate the IEPOX ring opening reaction. Current models consider only H^+ and HSO_4^- activity (McNeill et al., 2012; Pye et al., 2013), likely owing to the lack of experimental data describing the NH_4^+-initiated reaction with IEPOX, e.g., kinetic coefficients like $k_{NH_4^+}$. Thus, model predictions of a strong relationship between IEPOX-derived OA and particle acidity are contrary to both the results shown here and those observed in the Southeast USA (discounting caveats).

Future experimental and modeling studies should consider the NH_4^+ activity of a particle, in addition to the H^+ and HSO_4^- activity, for a more-accurate representation of OA formation from IEPOX.

The production of amines, alongside other low-volatility organic compounds that constitute a greater fraction of the OA mass, from the NH_4^+ reaction with IEPOX has been demonstrated. An updated reaction mechanism appears in Scheme 2, in which NH_4^+ and H^+ are shown to donate a proton to the epoxide oxygen, followed by nucleophilic addition to form oxygenated hydrocarbons, amines, and organosulfates. The ability of NH_4^+ to catalyze an epoxide ring opening is not unprecedented, as NH_4^+ can protonate aldehydes to facilitate nucleophilic addition (Noziere et al., 2009), and the high ring strain of an epoxide should provide an even greater thermodynamic motivation for the reaction. Indeed, due to the strain of epoxides, ring opening is chemically-facile and may be promoted by a wide range of aqueous chemical species and conditions common in atmospheric aerosols, in addition to H^+ and NH_4^+. For example, Lewis acids such as iron (Fe^{3+}) (Iranpoor and Salehi, 1994) and copper (Cu^{2+}) (Muzart and Riahi, 1992) ions may be even stronger catalysts. Furthermore, the reaction may proceed with no added catalyst, e.g., in the presence of amines (Azizi and Saidi, 2005) or even hot water (60 °C) (Wang et al., 2008). The nucleophiles for these reactions may be water, amines or ammonia, thiols, sulfate ions, nitrate ion, halide ions, carboxylic acids, and alcohols (Iranpoor et al., 1996; Jacobsen et al., 1997; Clayden et al., 2001). Because of the diversity in the composition of atmospheric aerosols and fog/cloud droplets (Graedel and Weschler, 1981), the distribution of IEPOX-derived products in nature may be more complex and varied than currently believed.

Supplementary material related to this article is available online at http://www.atmos-chem-phys-discuss.net/13/27677/2013/ acpd-13-27677-2013-supplement.pdf.

References

Aiken, A. C., Decarlo, P. F., Kroll, J. H., Worsnop, D. R., Huffman, J. A., Docherty, K. S., Ulbrich, I. M., Mohr, C., Kimmel, J. R., Sueper, D., Sun, Y., Zhang, Q., Trimborn, A., Northway, M., Ziemann, P. J., Canagaratna, M. R., Onasch, T. B., Alfarra, M. R., Prevot, A. S. H., Dommen, J., Duplissy, J., Metzger, A., Baltensperger, U., and Jimenez, J. L.: O/C and OM/OC ratios of primary, secondary, and ambient organic aerosols with high-resolution time-of-flight aerosol mass spectrometry, Environ. Sci. Technol., 42, 4478–4485, doi:10.1021/es703009q, 2008.

Allan, J. D., Delia, A. E., Coe, H., Bower, K. N., Alfarra, M. R., Jimenez, J. L., Middlebrook, A. M., Drewnick, F., Onasch, T. B., and Canagaratna, M. R.: A generalised method for the extraction of chemically resolved mass spectra from aerodyne aerosol mass spectrometer data, J. Aerosol Sci., 35, 909–922, 2004.

Azizi, N. and Saidi, M. R.: Highly chemoselective addition of amines to epoxides in water, Org. Lett., 7, 3649–3651, doi:10.1021/ol051220q, 2005.

Bates, K. H., Crounse, J. D., St. Clair, J., Nguyen, T. B., Bennett, N. B., Stoltz, B. M., Seinfeld, J. H., and Wennberg, P. O.: Rates and products of gas phase OH-initiated oxidation of isoprene epoxydiols (IEPOX), J. Phys. Chem., in preparation, 2013.

Biskos, G., Paulsen, D., Russell, L. M., Buseck, P. R., and Martin, S. T.: Prompt deliquescence and efflorescence of aerosol nanoparticles, Atmos. Chem. Phys., 6, 4633–4642, doi:10.5194/acp-6-4633-2006, 2006.

Bones, D. L., Henricksen, D. K., Mang, S. A., Gonsior, M., Bateman, A. P., Nguyen, T. B., Cooper, W. J., and Nizkorodov, S. A.: Appearance of strong absorbers and fluorophores in limonene-O_3 secondary organic aerosol due to NH_4^+-mediated chemical aging over long time scales, J. Geophys. Res., 115, D05203, doi:10.1029/2009JD012864, 2010.

Full Screen / Esc

Printer-friendly Version

Interactive Discussion

Full Screen / Esc

Printer-friendly Version

Interactive Discussion

Budisulistiorini, S. H., Canagaratna, M. R., Croteau, P. L., Marth, W. J., Baumann, K., Edgerton, E. S., Shaw, S. L., Knipping, E. M., Worsnop, D. R., Jayne, J. T., Gold, A., and Surratt, J. D.: Real-time continuous characterization of secondary organic aerosol derived from isoprene epoxydiols in downtown Atlanta, Georgia, using the Aerodyne aerosol chemical speciation monitor, Environ. Sci. Technol., 47, 5686–5694, doi:10.1021/es400023n, 2013.

Carlton, A. G. and Turpin, B. J.: Particle partitioning potential of organic compounds is highest in the Eastern US and driven by anthropogenic water, Atmos. Chem. Phys. Discuss., 13, 12743–12770, doi:10.5194/acpd-13-12743-2013, 2013.

Cavdar, H. and Saracoglu, N.: Ring opening of epoxides with $NaHSO_4$: isolation of β-hydroxy sulfate esters and an effective synthesis for trans-diols, Tetrahedron, 65, 985–989, 2009.

Chan, M. N., Surratt, J. D., Claeys, M., Edgerton, E. S., Tanner, R. L., Shaw, S. L., Zheng, M., Knipping, E. M., Eddingsaas, N. C., Wennberg, P. O., and Seinfeld, J. H.: Characterization and quantification of isoprene-derived epoxydiols in ambient aerosol in the Southeastern United States, Environ. Sci. Technol., 44, 4590–4596, doi:10.1021/es100596b, 2010.

Clayden, J., Greeves, N., Warren, S., and Wothers, P.: Organic Chemistry, Oxford University Press, ISBN 978-380-319-850346-850340, 386 pp., 2001.

Clegg, S. L., Brimblecombe, P., and Wexler, A. S.: Thermodynamic model of the system H^+-NH_4^+-SO_4^{2-}-NO_3-H_2O at tropospheric temperatures, J. Phys. Chem. A, 102, 2137–2154, doi:10.1021/jp973042r, 1998.

Crounse, J. D., McKinney, K. A., Kwan, A. J., and Wennberg, P. O.: Measurement of gas-phase hydroperoxides by chemical ionization mass spectrometry, Anal. Chem., 78, 6726–6732, doi:10.1021/ac0604235, 2006.

Docherty, K. S., Jaoui, M., Corse, E., Jimenez, J. L., Offenberg, J. H., Lewandowski, M., and Kleindienst, T. E.: Collection efficiency of the aerosol mass spectrometer for chamber-generated secondary organic aerosols, Aerosol Sci. Tech., 47, 294–309, 2013.

Eddingsaas, N. C., VanderVelde, D. G., and Wennberg, P. O.: Kinetics and products of the acid-catalyzed ring-opening of atmospherically relevant butyl epoxy alcohols, J. Phys. Chem. A, 114, 8106–8113, doi:10.1021/jp103907c, 2010.

EPA: Estimation Programs Interface for Microsoft Mindows XP v4.0; US EPA, 2008.

Ervens, B. and Volkamer, R.: Glyoxal processing by aerosol multiphase chemistry: towards a kinetic modeling framework of secondary organic aerosol formation in aqueous particles, Atmos. Chem. Phys., 10, 8219–8244, doi:10.5194/acp-10-8219-2010, 2010.

Froyd, K. D., Murphy, S. M., Murphy, D. M., de Gouw, J. A., Eddingsaas, N. C., and Wennberg, P. O.: Contribution of isoprene-derived organosulfates to free tropospheric aerosol mass, P. Natl. Acad. Sci. USA, 107, 21360–21365, doi:10.1073/pnas.1012561107, 2010.

Graedel, T. E. and Weschler, C. J.: Chemistry within aqueous atmospheric aerosols and raindrops, Rev. Geophys., 19, 505–539, doi:10.1029/RG019i004p00505, 1981.

Gregoire, P.: Implications of Ambient Ammonia on Aerosol Acidity and Reactive Nitrogen Measurements, M.S., Department of Chemistry, University of Toronto, Toronto, Ontario, Canada, 82 pp., 2013.

Griffith, D. W. T.: Synthetic calibration and quantitative analysis of gas-phase FT-IR spectra, Appl. Spectrosc., 50, 59–70, 1996.

Hatch, L. E., Creamean, J. M., Ault, A. P., Surratt, J. D., Chan, M. N., Seinfeld, J. H., Edgerton, E. S., Su, Y., and Prather, K. A.: Measurements of isoprene-derived organosulfates in ambient aerosols by aerosol time-of-flight mass spectrometry – Part 2: Temporal variability and formation mechanisms, Environ. Sci. Technol., 45, 8648–8655, doi:10.1021/es2011836, 2011.

Hennigan, C. J., Bergin, M. H., Dibb, J. E., and Weber, R. J.: Enhanced secondary organic aerosol formation due to water uptake by fine particles, Geophys. Res. Lett., 35, L18801, doi:10.1029/2008GL035046, 2008.

Hennigan, C. J., Bergin, M. H., Russell, A. G., Nenes, A., and Weber, R. J.: Gas/particle partitioning of water-soluble organic aerosol in Atlanta, Atmos. Chem. Phys., 9, 3613–3628, doi:10.5194/acp-9-3613-2009, 2009.

Hu, D., Qiao, L., Chen, J., Ye, X., Yang, X., Cheng, T., and Fang, W.: Hygroscopicity of inorganic aerosols: size and relative humidity effects on the growth factor, Aerosol Air. Qual. Res., 10, 255–264, 2010.

Ip, H. S. S., Huang, X. H. H., and Yu, J. Z.: Effective Henry's law constants of glyoxal, glyoxylic acid, and glycolic acid, Geophys. Res. Lett., 36, L01802, doi:10.1029/2008gl036212, 2009.

Iranpoor, N. and Salehi, P.: Highly efficient, regio-and stereoselective alcoholysis of epoxides catalyzed with iron (iii) chloride, Synthesis, 1994, 1152–1154, 1994.

Iranpoor, N., Tarrian, T., and Movahedi, Z.: $FeCl_3 \cdot 6H_2O$ supported on SiO_2 catalysed ring opening of epoxides with alcohols, acetic acid, water, chloride, bromide and nitrate ions, Synthesis, 1996, 1473–1476, 1996.

Title Page

Abstract | Introduction

Conclusions | References

Tables | Figures

◄ | ►◄

◄ | ►

Back | Close

Full Screen / Esc

Printer-friendly Version

Interactive Discussion

Jacobsen, E. N., Kakiuchi, F., Konsler, R. G., Larrow, J. F., and Tokunaga, M.: Enantioselective catalytic ring opening of epoxides with carboxylic acids, Tetrahedron Lett., 38, 773–776, 1997.

Kampf, C. J., Waxman, E. M., Slowik, J. G., Dommen, J., Pfaffenberger, L., Praplan, A. P., Prévôt, A. S. H., Baltensperger, U., Hoffmann, T., and Volkamer, R.: Effective Henry's law partitioning and the salting constant of glyoxal in aerosols containing sulfate, Environ. Sci. Technol., 47, 4236–4244, doi:10.1021/es400083d, 2013.

Lee, C.-T. and Hsu, W.-C.: The measurement of liquid water mass associated with collected hygroscopic particles, J. Aerosol. Sci., 31, 189–197, 2000.

Lin, Y.-H., Zhang, Z., Docherty, K. S., Zhang, H., Budisulistiorini, S. H., Rubitschun, C. L., Shaw, S. L., Knipping, E. M., Edgerton, E. S., Kleindienst, T. E., Gold, A., and Surratt, J. D.: Isoprene epoxydiols as precursors to secondary organic aerosol formation: acid-catalyzed reactive uptake studies with authentic compounds, Environ. Sci. Technol., 46, 250–258, doi:10.1021/es202554c, 2012.

Lin, Y.-H., Knipping, E. M., Edgerton, E. S., Shaw, S. L., and Surratt, J. D.: Investigating the influences of SO_2 and NH_3 levels on isoprene-derived secondary organic aerosol formation using conditional sampling approaches, Atmos. Chem. Phys., 13, 8457–8470, doi:10.5194/acp-13-8457-2013, 2013.

Loza, C. L., Chan, A. W. H., Galloway, M. M., Keutsch, F. N., Flagan, R. C., and Seinfeld, J. H.: Characterization of vapor wall loss in laboratory chambers, Environ. Sci. Technol., 44, 5074–5078, doi:10.1021/es100727v, 2010.

Loza, C. L., Chhabra, P. S., Yee, L. D., Craven, J. S., Flagan, R. C., and Seinfeld, J. H.: Chemical aging of *m*-xylene secondary organic aerosol: laboratory chamber study, Atmos. Chem. Phys., 12, 151–167, doi:10.5194/acp-12-151-2012, 2012.

Martin, S. T.: Phase transitions of aqueous atmospheric particles, Chem. Rev., 100, 3403–3453, 2000.

Matthew, B. M., Middlebrook, A. M., and Onasch, T. B.: Collection efficiencies in an Aerodyne aerosol mass spectrometer as a function of particle phase for laboratory generated aerosols, Aerosol Sci. Tech., 42, 884–898, doi:10.1080/02786820802356797, 2008.

McNeill, V. F., Woo, J. L., Kim, D. D., Schwier, A. N., Wannell, N. J., Sumner, A. J., and Barakat, J. M.: Aqueous-phase secondary organic aerosol and organosulfate formation in atmospheric aerosols: a modeling study, Environ. Sci. Technol., 46, 8075–8081, 2012.

Title Page

Abstract | Introduction

Conclusions | References

Tables | Figures

◄ | ►

◄ | ►

Back | Close

Full Screen / Esc

Printer-friendly Version

Interactive Discussion

Minerath, E. C., Casale, M. T., and Elrod, M. J.: Kinetics feasibility study of alcohol sulfate esterification reactions in tropospheric aerosols, Environ. Sci. Technol., 42, 4410–4415, doi:10.1021/es8004333, 2008.

Minerath, E. C., Schultz, M. P., and Elrod, M. J.: Kinetics of the reactions of isoprene-derived epoxides in model tropospheric aerosol solutions, Environ. Sci. Technol., 43, 8133–8139, doi:10.1021/es902304p, 2009.

Muzart, J. and Riahi, A.: Palladium- and light-enhanced ring-opening of oxiranes by copper chloride, J. Organomet. Chem., 433, 323–336, 1992.

Nguyen, T. B., Lee, P. B., Updyke, K. M., Bones, D. L., Laskin, J., Laskin, A., and Nizkorodov, S. A.: Formation of nitrogen- and sulfur-containing light-absorbing compounds accelerated by evaporation of water from secondary organic aerosols, J. Geophys. Res., 117, D01207, doi:10.1029/2011jd016944, 2012.

Nguyen, T. B., Laskin, A., Laskin, J., and Nizkorodov, S. A.: Brown carbon formation from ketoaldehydes of biogenic monoterpenes, Faraday Discuss., 165, doi:10.1039/c3fd00036b, 2013.

Noziere, B., Dziedzic, P., and Cordova, A.: Products and kinetics of the liquid-phase reaction of glyoxal catalyzed by ammonium ions (NH_4^+), J. Phys. Chem. A, 113, 231–237, doi:10.1021/jp8078293, 2009.

Paulot, F., Crounse, J. D., Kjaergaard, H. G., Kroll, J. H., Seinfeld, J. H., and Wennberg, P. O.: Isoprene photooxidation: new insights into the production of acids and organic nitrates, Atmos. Chem. Phys., 9, 1479–1501, doi:10.5194/acp-9-1479-2009, 2009a.

Paulot, F., Crounse, J. D., Kjaergaard, H. G., Kurten, A., St. Clair, J. M., Seinfeld, J. H., and Wennberg, P. O.: Unexpected epoxide formation in the gas-phase photooxidation of isoprene, Science, 325, 730–733, doi:10.1126/science.1172910, 2009b.

Pye, H. O. T., Pinder, R. W., Piletic, I. R., Xie, Y., Capps, S. L., Lin, Y.-H., Surratt, J. D., Zhang, Z., Gold, A., Luecken, D. J., Hutzell, W. T., Jaoui, M., Offenberg, J. H., Kleindienst, T. E., Lewandowski, M., and Edney, E. O.: Epoxide pathways improve model predictions of isoprene markers and reveal key role of acidity in aerosol formation, Environ. Sci. Technol., 47, 11056–11064, doi:10.1021/es402106h, 2013.

Reuss, J.: Chemical and biological relationships relevant to the effect of acid rainfall on the soil-plant system, Water Air Soil Pollut., 7, 461–478, doi:10.1007/bf00285545, 1977.

Robinson, N. H., Hamilton, J. F., Allan, J. D., Langford, B., Oram, D. E., Chen, Q., Docherty, K., Farmer, D. K., Jimenez, J. L., Ward, M. W., Hewitt, C. N., Barley, M. H., Jenkin, M. E.,

Rickard, A. R., Martin, S. T., McFiggans, G., and Coe, H.: Evidence for a significant proportion of Secondary Organic Aerosol from isoprene above a maritime tropical forest, Atmos. Chem. Phys., 11, 1039–1050, doi:10.5194/acp-11-1039-2011, 2011.

Rothman, L. S., Gordon, I. E., Barbe, A., Benner, D. C., Bernath, P. F., Birk, M., Boudon, V., Brown, L. R., Campargue, A., and Champion, J.-P.: The HITRAN 2008 molecular spectroscopic database, J. Quant. Spectrosc. Ra., 110, 533–572, 2009.

Sareen, N., Schwier, A. N., Shapiro, E. L., Mitroo, D., and McNeill, V. F.: Secondary organic material formed by methylglyoxal in aqueous aerosol mimics, Atmos. Chem. Phys., 10, 997–1016, doi:10.5194/acp-10-997-2010, 2010.

Seinfeld, J. H. and Pandis, S. N.: Atmospheric Chemistry and Physics: from Air Pollution to Climate Change, Wiley, 2006.

Solomons, T. W. G. and Fryhle, C. B.: Organic Chemistry, 8th edn., John Wiley & Sons, Inc., Hoboken, NJ, 2004.

St. Clair, J. M., McCabe, D. C., Crounse, J. D., Steiner, U., and Wennberg, P. O.: Chemical ionization tandem mass spectrometer for the in situ measurement of methyl hydrogen peroxide, Rev. Sci. Instrum., 81, 094102–094106, 2010.

Surratt, J., Chan, A. W. H., Eddingsaas, N. C., Chan, M., Loza, C. L., Kwan, A. J., Hersey, S. P., Flagan, R. C., Wennberg, P. O., and Seinfeld, J. H.: Reactive intermediates revealed in secondary organic aerosol formation from isoprene, P. Natl. Acad. Sci. USA, 107, 6640–6645, 2010.

Surratt, J. D., Lewandowski, M., Offenberg, J. H., Jaoui, M., Kleindienst, T. E., Edney, E. O., and Seinfeld, J. H.: Effect of acidity on secondary organic aerosol formation from isoprene, Environ. Sci. Technol., 41, 5363–5369, 2007.

Wang, Z., Cui, Y.-T., Xu, Z.-B., and Qu, J.: Hot water-promoted ring-opening of epoxides and aziridines by water and other nucleopliles, J. Org. Chem., 73, 2270–2274, doi:10.1021/es902304p, 2008.

Xiong, J. Q., Zhong, M., Fang, C., Chen, L. C., and Lippmann, M.: Influence of organic films on the hygroscopicity of ultrafine sulfuric acid aerosol, Environ. Sci. Technol., 32, 3536–3541, 1998.

Yu, G., Bayer, A. R., Galloway, M. M., Korshavn, K. J., Fry, C. G., and Keutsch, F. N.: Glyoxal in aqueous ammonium sulfate solutions: products, kinetics and hydration effects, Environ. Sci. Technol., 45, 6336–6342, doi:10.1021/es200989n, 2011.

Title Page

Abstract | Introduction

Conclusions | References

Tables | Figures

|◄ | ►|

◄ | ►

Back | Close

Full Screen / Esc

Printer-friendly Version

Interactive Discussion

Zhang, Z., Lin, Y.-H., Zhang, H., Surratt, J. D., Ball, L. M., and Gold, A.: Technical Note: Synthesis of isoprene atmospheric oxidation products: isomeric epoxydiols and the rearrangement products *cis*- and *trans*-3-methyl-3,4-dihydroxytetrahydrofuran, Atmos. Chem. Phys., 12, 8529–8535, doi:10.5194/acp-12-8529-2012, 2012.

Zuend, A., Marcolli, C., Luo, B. P., and Peter, T.: A thermodynamic model of mixed organic-inorganic aerosols to predict activity coefficients, Atmos. Chem. Phys., 8, 4559–4593, doi:10.5194/acp-8-4559-2008, 2008.

Zuend, A., Marcolli, C., Booth, A. M., Lienhard, D. M., Soonsin, V., Krieger, U. K., Topping, D. O., McFiggans, G., Peter, T., and Seinfeld, J. H.: New and extended parameterization of the thermodynamic model AIOMFAC: calculation of activity coefficients for organic-inorganic mixtures containing carboxyl, hydroxyl, carbonyl, ether, ester, alkenyl, alkyl, and aromatic functional groups, Atmos. Chem. Phys., 11, 9155–9206, doi:10.5194/acp-11-9155-2011, 2011.

Title Page

Abstract | Introduction

Conclusions | References

Tables | Figures

|◀ | ▶|

◀ | ▶

Back | Close

Full Screen / Esc

Printer-friendly Version

Interactive Discussion

Table 1. Summary of results from representative reactive uptake experiments onto ammonium sulfate seeds. Mean results from Lin et al. (2012) are shown for comparison.

Exp. Index	IEPOX Isomer	Seed Composition	RH (%)	Particle pH^a	Seed ($\mu g\,m^{-3}$)	P_{LWC} ($g\,m^{-3}$)	C_{OA}/C_{IEPOX}	$\Phi_{OA/IEPOX}$ ($M\,atm^{-1}$)
1	*cis*	$(NH_4)_2SO_4$	3	–	70	$< 1 \times 10^{-6}$	5.04×10^{-4}	–
2	*cis*	$(NH_4)_2SO_4$	42	3.67	91	3.74×10^{-5}	0.102	1.15×10^8
3	*cis*	$(NH_4)_2SO_4$	50	3.74	92	4.79×10^{-5}	0.118	1.01×10^8
4	*cis*	$(NH_4)_2SO_4$	86	3.90	81	5.68×10^{-5}	0.179	4.00×10^7
5	*trans*	$(NH_4)_2SO_4$	2	–	65	$< 1 \times 10^{-6}$	4.74×10^{-4}	–
6	*trans*	$(NH_4)_2SO_4$	39	3.65	82	3.44×10^{-5}	0.090	1.06×10^8
7	*trans*	$(NH_4)_2SO_4$	57	3.77	89	4.64×10^{-5}	0.095	8.44×10^7
8	*trans*	$(NH_4)_2SO_4$	81	3.88	88	6.14×10^{-5}	0.115	7.66×10^7
9	*trans*	$(NH_4)_2SO_4$ + NaOH, pH = 7	70	~ 5.5	84	5.33×10^{-5}	0.090	6.89×10^7
Lin et al. (2012)	*cis*	$MgSO_4$ + H_2SO_4 (1 : 1)	< 5	~ −10	48	1.62×10^{-5b}	0.058	1.47×10^8

^{a} Modeled pH using E-AIM and AIOMFAC models (the value from (Lin et al., 2012) is $a_{molality}$-based pH), see text (Sect. 3.1.2).

^{b} Based on hygroscopicity of H_2SO_4 at RH 5 %, assumed growth factor 1.15 (Xiong et al., 1998).

Fig. 1. Typical uptake experiment results as a function of time, shown for *trans* isomer, at dry (top) and humid (bottom) conditions with the corresponding percent liquid water content (LWC). The solid black line indicates when IEPOX injection stopped and the mixture was allowed to equilibrate. Double y-axes correspond to traces of the same color.

Title Page

Abstract Introduction

Conclusions References

Tables Figures

◄ ►

◄ ►

Back Close

Full Screen / Esc

Printer-friendly Version

Interactive Discussion
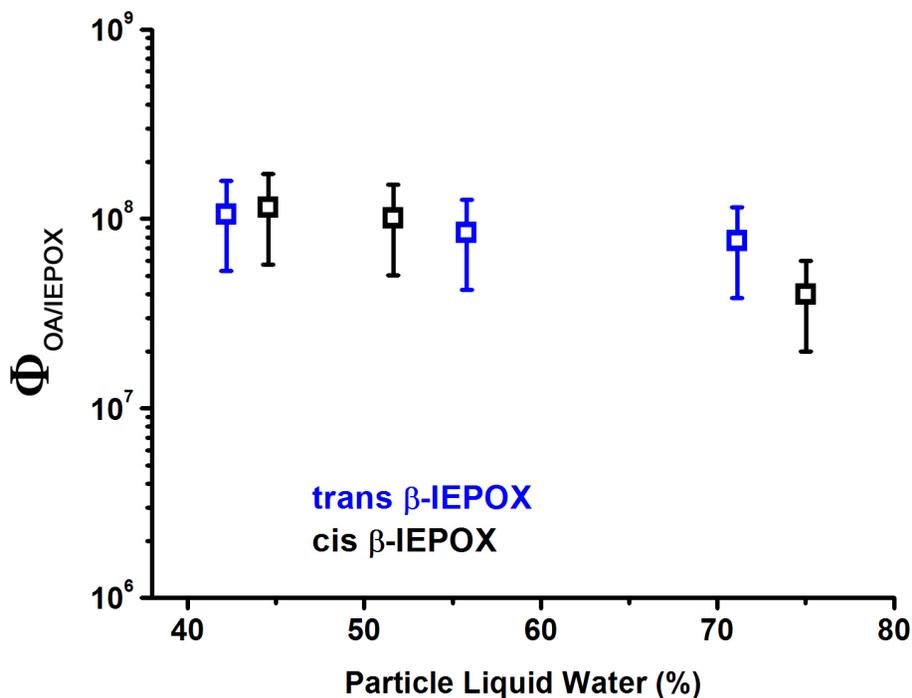
Fig. 2. Reactive partitioning coefficients ($\Phi_{OA/IEPOX}$) during the gas-phase IEPOX injection phase for the *trans* and *cis* isomers as a function of the particle liquid water concentration. Error bars indicate an estimated combined 50 % error.
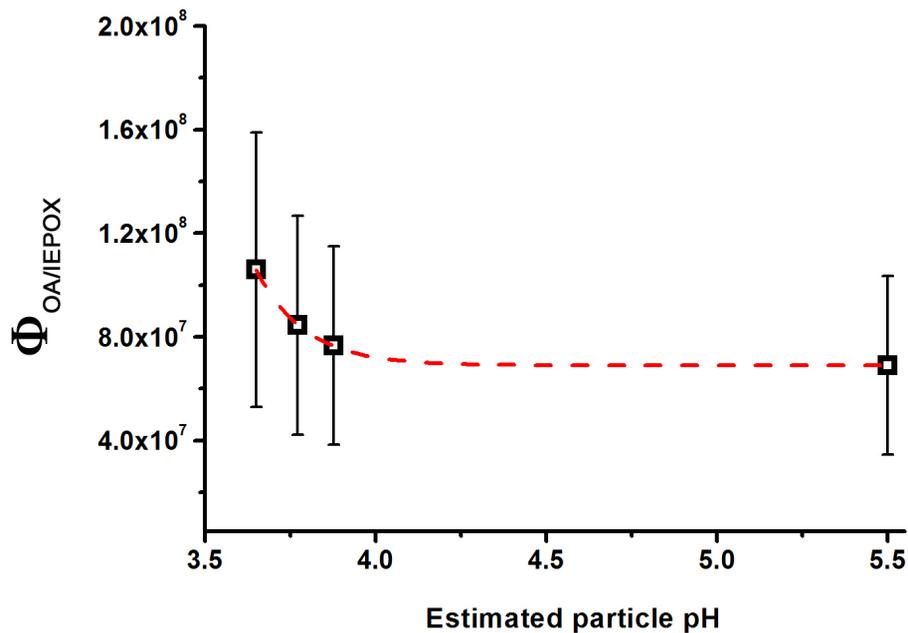
Fig. 3. $\Phi_{OA/IEPOX}$ for the *trans* β-IEPOX isomer as a function of the modeled particle pH.

Full Screen / Esc
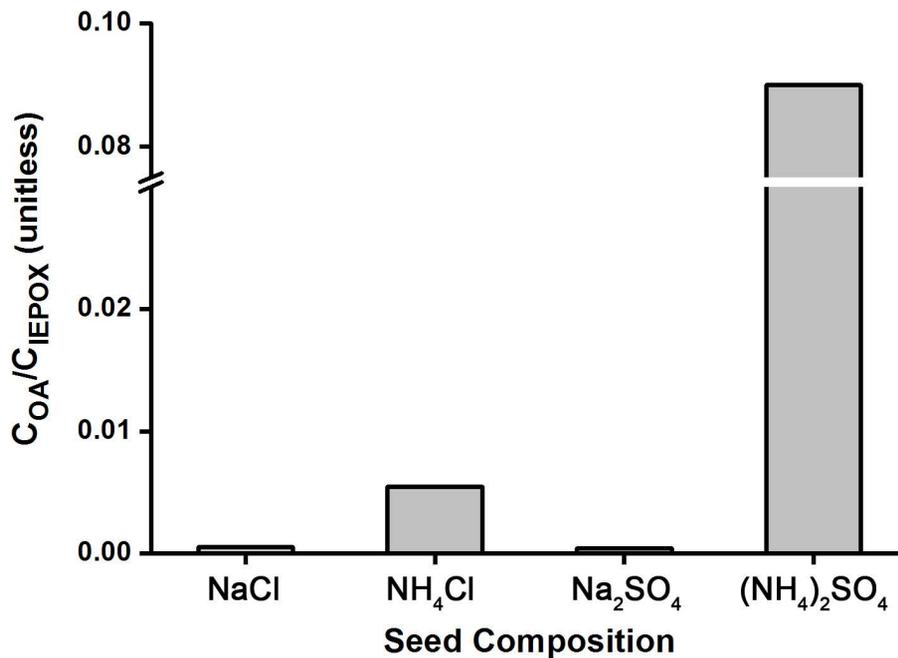
Fig. 4. Ratio of organic aerosol produced to gas-phase *trans β*-IEPOX injected for seeds of various composition (RH 60–85 %).
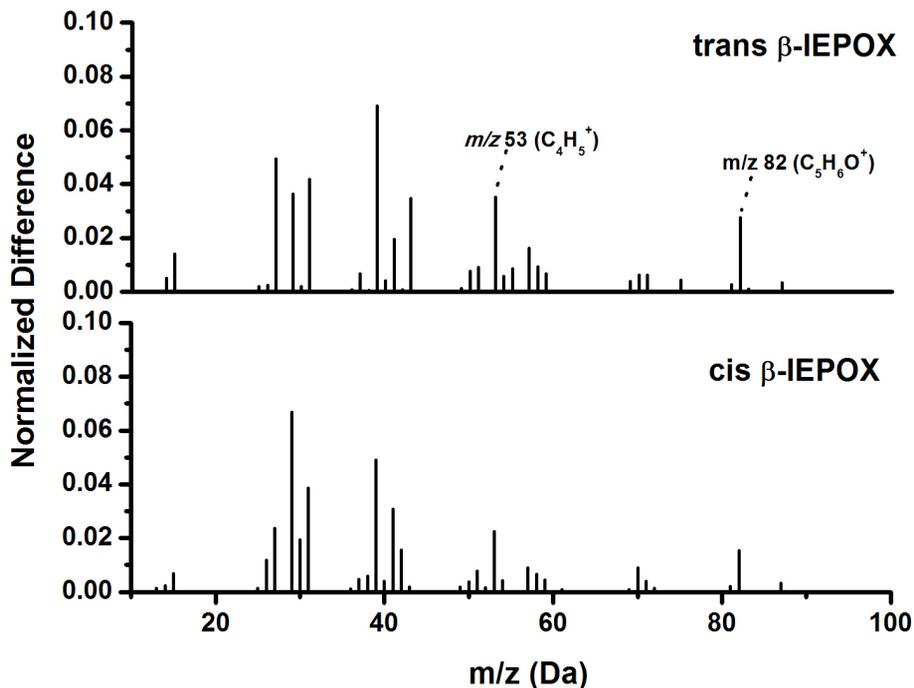
Fig. 5. ToF-AMS normalized difference spectra (composition at peak OA growth – composition during seed injection), showing the organic composition of the OA produced by reactive uptake of the *trans* and *cis* isomers. Select nominal mass ions suggested to be IEPOX-derived OA tracers are labeled.
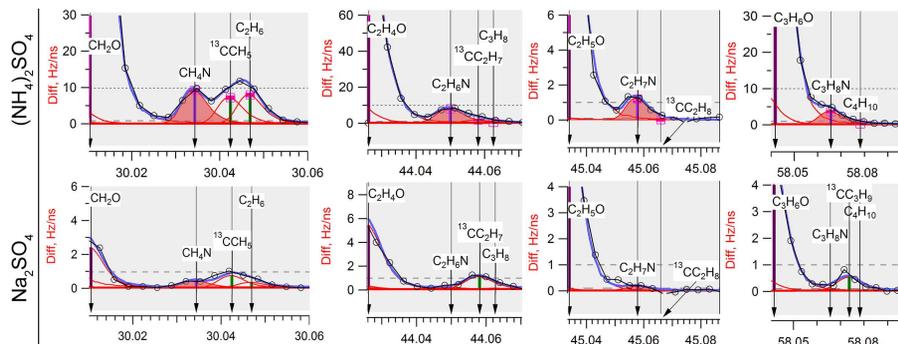
Fig. 6. ToF-AMS difference spectra (open–closed chopper) showing organic nitrogen (amine) fragments from the reactive uptake of *trans* β-IEPOX onto AS vs. Na_2SO_4 seeds. Similar fragments were observed for *cis* β-IEPOX using NH_4^+-based seeds and not observed in Na^+-based seeds.
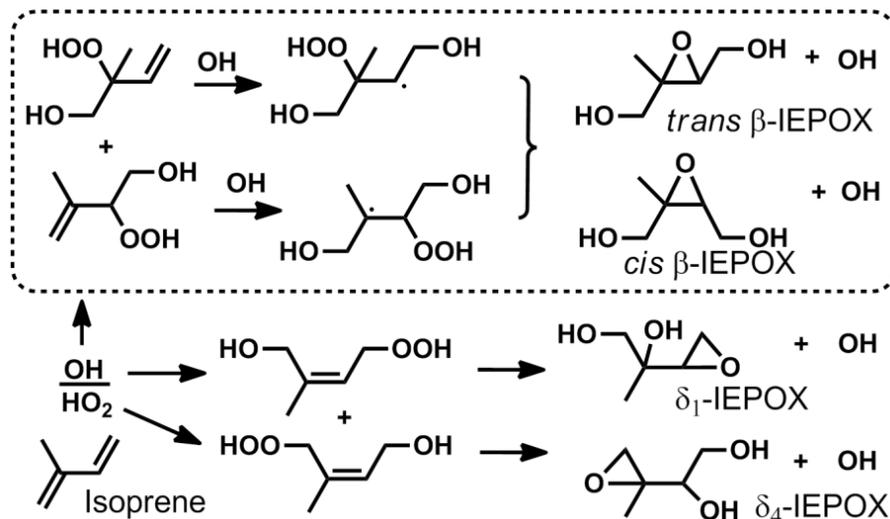
Scheme 1. Formation of IEPOX isomers, from relevant isoprene hydroxy hydroperoxide precursors, in the low-NO photooxidation of isoprene. The expected dominant pathway is shown inside the box. The naming convention is based on Paulot et al. (2009b).

Title Page

Abstract | Introduction

Conclusions | References

Tables | Figures

|◄ | ►|

◄ | ►

Back | Close

Full Screen / Esc

Printer-friendly Version

Interactive Discussion
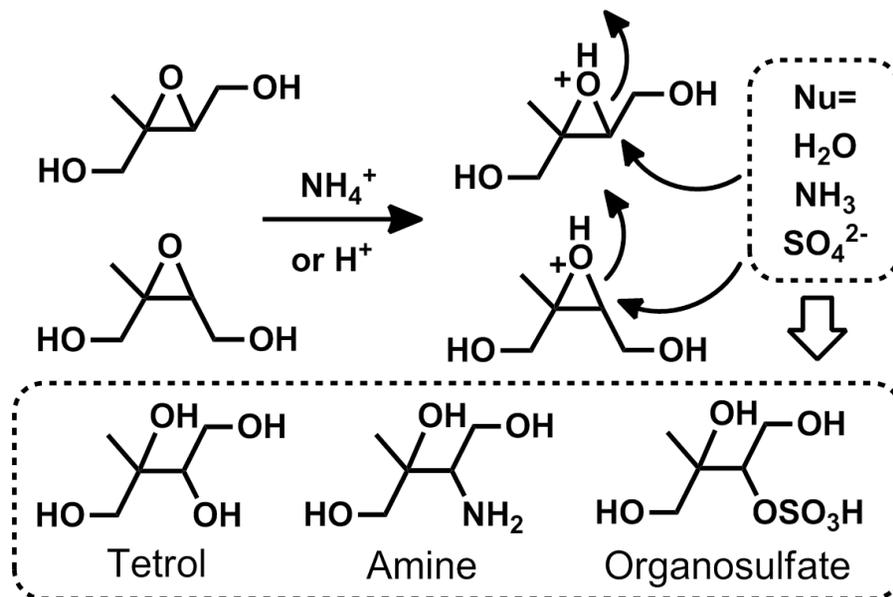
Scheme 2. Addition of inorganic nucleophiles in the aqueous NH_4^+ and H^+-catalyzed ring opening of IEPOX to form low-volatility organic compounds.